Adsorption (2009) 15: 390–405
DOI 10.1007/s10450-009-9156-y

Adsorption of crystal violet dye from aqueous solution using mesoporous materials synthesized at room temperature

P. Monash · G. Pugazhenthi

Received: 28 July 2008 / Revised: 16 January 2009 / Accepted: 9 February 2009 / Published online: 26 February 2009

Abstract In this work, batch adsorption experiments are carried out for crystal violet dye using mesoporous MCM-41 synthesized at room temperature and sulfate modified MCM-41 prepared by impregnation method using H_2SO_4 as sulfatising agent. The surface characteristics, pore structure, bonding behavior and thermal degradation of both the MCM-41 samples are characterized by nitrogen adsorption/desorption isotherms, X-ray diffraction (XRD) patterns, Fourier transform infrared (FT-IR) spectroscopy and thermo gravimetric analysis (TGA). The adsorption isotherm, kinetics and thermodynamic parameters are investigated for crystal violet (CV) dye using the calcined and sulfated MCM-41. Results are analysed using Langmuir, Freundlich and Redlich-Peterson isotherm models. It is found that the Freundlich model is an appropriate model to explain the adsorption isotherm. The highest adsorption capacity achieved is found to be 3.4×10^{-4} mol g^{-1} for the sulfated MCM-41. The percentage removal of crystal violet dye increases with increase in the pH for both the MCM-41 adsorbents. Kinetics of adsorption is found to follow the second-order rate equation. From the thermodynamic investigation, it is evident that the adsorption is exothermic in nature.

Keywords Adsorption · Crystal violet · MCM-41 · Sulfated · Isotherm

Abbreviations

MCM Mobil Composition of Matter

P. Monash · G. Pugazhenthi (✉)
Department of Chemical Engineering, Indian Institute of Technology Guwahati, Guwahati 781039, India
e-mail: pugal@iitg.ernet.in
url: http://www.iitg.ernet.in/chemeng/gpugal.html

CV	Crystal Violet
CTAB	Cetyltrimethylammonium Bromide
TEOS	Tetraethylorthosilicate
a_0	Unit cell Parameter (nm)
C_0	Initial concentration (mol dm^{-3})
C_e	Concentration at equilibrium (mol dm^{-3})
C_t	Concentration at time t (mol dm^{-3})
d_{100}	d-Spacing (nm)
D_p	Internal pore diameter (nm)
d_{XRD}	crystallite size (nm)
G^0	Free energy (KJ mol^{-1})
H^0	Enthalpy (KJ mol^{-1})
k_1	Pseudo-first-order rate constant (min^{-1})
k_2	Pseudo-second-order rate constant (gmol^{-1} min^{-1})
k_d	Diffusion coefficient (dimensionless)
K_F	Freundlich isotherm constant (mol/g(dm^3/mol)$^{1/n}$)
K_L	Langmuir constant (dm^3 mol^{-1})
K_{RP}	Redlich-Peterson constants (mol g^{-1})
m	Mass of the adsorbent (g)
n	Adsorption intensity (dimensionless)
q_e	Amount of dye adsorbed at equilibrium (mol g^{-1})
$Q_{\max}$	Maximum adsorption capacity (mol g^{-1})
S^0	Entropy (KJ mol^{-1} K^{-1})
S_{BET}	BET surface area (m^2 g^{-1})
V	Volume (dm^3)
V_{mes}	Mesoporous volume (cm^3 g^{-1})

Greek letters

β	Full width at half maximum (degrees)
θ	Angle of diffraction (degrees)
λ	Wavelength (nm)
$\lambda_{\max}$	Maximum absorbance wavelength (nm)

1 Introduction

Many industries, such as textile, paper, printing, leather, food, cosmetics, etc., use dyes to color their products, which generate a considerable amount of colored wastewater. The color present in the effluent creates lots of environmental issues. The removal of color from the synthetic dyes is of a great concern nowadays, because many dyes and their degradation products are toxic and carcinogenic, posing a serious hazard to aquatic living organisms (Crini 2006; Garg et al. 2004). Crystal violet is most widely used for dyeing and also being used as a biological stain, dermatological agent, veterinary medicine, etc. (Adak et al. 2005). Generally, the treatments of the dyestuff effluents can be classified into three major categories, namely, biological, chemical and physical treatment. Each of the above treatment methods have their own merits and demerits and are reported in many literatures (Crini 2006; Garg et al. 2004). Among the various treatment methods, adsorption is found to be the versatile process and gives best results in the treatment of the colored dyestuff effluents. Most of the investigations are based on commercial activated carbon and activated carbon derived from various sources and found to be more effective for color removal (Tsang et al. 2007). Even though activated carbon showed advantages, the main drawback of the activated carbon is the cost and difficulty in regeneration (Liu et al. 2007). Non-conventional low-cost adsorbents, including natural materials, clays, biosorbents, and waste materials are also successfully applied for the treatment of the dye effluents (Crini and Badot 2008; Namasivayam and Sumithra 2005; Garg et al. 2004).

Most of the clay adsorbents containing aluminosilicates in different ratios, containing specific surface charges make the dye to adsorb on the clays. Recently, mesoporous aluminosilicates produced by the mobil oil corporation, called MCM (Mobil Composition of Matter), shows very interesting properties. High surface area and nanometer sized pore of the MCM, especially MCM-41, makes it an ideal material for catalyst applications. It is also used for testing various adsorption and diffusion models because of its high pore volume. Most of the adsorption studies are concentrated on gases and only a few works have been reported for liquid-phase systems (Zhao et al. 1996; Juang et al. 2006). The main advantage of MCM-41 is that it can be regenerated by simple washing with alkaline or acid solution to recover the adsorbents and adsorbed dyes (Juang et al. 2006). Only few literatures are available on the adsorption of dyes on MCM-41 synthesized at high temperature using autoclave reactor (Ho et al. 2003; Juang et al. 2006; Wang and Li 2006; Lee et al. 2007). Parida and Rath (2006) have reported that the acidity of MCM-41 was increased by the incorporation of sulfate ions into the structure. The sulfated MCM-41 may be used as an effective adsorbent for the treatment of dyes. No literatures are found, to the best of the authors knowledge, on the removal of dyes using sulfated MCM-41 as an adsorbent.

The main objective of the present work is to investigate the room temperature synthesized MCM-41 and the sulfated MCM-41 as a suitable candidate for the removal of crystal violet dye from aqueous solution. The synthesized materials are characterized with nitrogen adsorption/desorption isotherms, XRD, FTIR and TGA. The influence of pH and temperature on adsorption characteristics of both calcined and sulfated MCM-41 is studied and the experimental data obtained from the equilibrium studies are fitted to Langmuir, Freundlich and Redlich-Peterson adsorption models. In addition, a kinetic study is also carried out to determine the adsorption mechanism and a thermodynamic study is made to get a clear knowledge of the adsorption mechanism.

2 Materials and methods

2.1 Materials

Tetraethylorthosilicate (TEOS) and *n*-cetyltrimethylammonium bromide (CTAB, chemical formula = $C_{19}H_{42}BrN$, Mol. wt. = 364.45) were purchased from Merck (Germany) and S.D Fine Chemicals (Mumbai, India), respectively. Ammonium hydroxide (25 wt.%), ethanol, sodium hydroxide (NaOH), sulphuric acid (H_2SO_4) and hydrochloric acid (HCl) were procured from Merck (I) Ltd (Mumbai, India). Crystal violet (C. I. 42555, chemical formula = $C_{25}H_{30}N_3Cl$, Mol. wt. = 407.99) was purchased from Loba Chemie-India (India). All the chemicals were used as received. Water used in the preparation of MCM-41 and dye solution was collected from the Millipore System.

2.2 Adsorbent synthesis

2.2.1 Synthesis of MCM-41

Modified classical synthesis route was adopted for the preparation of MCM-41 under mild conditions interms of temperature and surfactant amount (Kumar et al. 2001). The material was synthesized by dissolving 2.4 g of CTAB in 120 ml of Millipore water at room temperature and stirred continuously using a laboratory stirrer until a clear homogeneous solution was obtained. Then 10.2 ml of 25 wt.% aqueous ammonia was added into the homogeneous solution and the mixture was stirred for 5 min. A required amount of TEOS was added drop by drop into the above mixture with continuous stirring. The solution became milky and a gel was formed due to the hydrolysis of TEOS at room temperature. The molar composition of the gel was 1 M TEOS: 3.089 M NH_3: 0.1358 M CTAB: 137.54 M H_2O. The mixture was stirred overnight to achieve the condensation of

the mesostructured hybrid material. The white precipitate formed was filtered and washed consecutively with Millipore water and ethanol. Finally, the solid product was calcined at 550 °C in air atmosphere for 5 h in order to remove the trapped surfactant. The product before and after calcination were labeled as as-synthesized MCM-41 and calcined MCM-41, respectively.

2.2.2 *Synthesis of sulfated MCM-41*

A wet impregnation method was followed for the preparation of sulfated MCM-41, in which the impregnation of sulfate ion was done by using H_2SO_4 (Aquino et al. 2001). About 1 g of calcined MCM-41 sample was treated with 30 ml of 0.25 M H_2SO_4 (98% H_2SO_4) at room temperature for 2 h and heated at 70 °C until complete evaporation. The sample was again dried at 110 °C for 10 h and calcined at 550 °C for 5 h in a muffle furnace to get sulfated MCM-41.

2.3 Characterization of adsorbents

Thermo gravimetric analysis (TGA) was performed on the Mettler Toledo thermo gravimetric analyzer (TGA/SDTA 851® model). The measurements were carried out in air atmosphere from 25 °C to 970 °C with a heating rate of 10 °C min^{-1}. The X-ray diffraction (XRD) patterns were recorded in air atmosphere at room temperature on a Bruker AXS instrument equipped with Cu Kα (λ = 1.5406 °A) radiation operating at 40 kV and 40 mA between 2θ angle range of 0.5 and 10 ° with a scan speed of 0.02 ° s^{-1}. Nitrogen adsorption/desorption isotherms were measured at −196 °C using Beckmen-Coulter surface area analyzer (SA™ 3100 model). All the MCM-41 samples were degassed at 150 °C for 4 h, prior to the N_2 adsorption/desorption analysis. The surface area was calculated using a multipoint Brunauer-Emmett-Teller (BET) model. The pore size distribution was obtained through the Barrett, Joyner and Halenda (BJH) model using the desorption isotherms and the total pore volume was estimated at a relative pressure of 0.99, assuming full surface saturation with nitrogen. FT-IR spectra were recorded between 4000 and 450 cm^{-1} region using spectroscopic quality KBr powder with a Perkin-Elmer spectrometer (spectrum one model).

2.4 Adsorption isotherm studies

Adsorption isotherm studies were carried out using the above synthesized adsorbents by batch equilibrium technique. The dye was first dried at 100 °C for 2 h to remove the moisture. A stock solution having concentration of 9.804×10^{-4} M was prepared and the experimental solutions of the desired concentration were obtained by successive dilutions of the stock solution. For adsorption isotherm experiments, 50 ml of dye solution of known initial concentrations in the range of 2.45×10^{-5} to 6.13×10^{-4} M were shaken with 0.02 g of MCM-41 in an incubator shaker (Labtech®, Korea) at 100 rpm. The pH values of CV solutions were not adjusted except for investigating the effect of pH on CV adsorption. The solution and solid phase were separated by centrifugation at 8000 rpm for 30 min in a high speed refrigerated table top centrifuge (Sigma Laborzentrifugen Gmbh, Model 4k15C). About 10 ml of the supernatant was collected without disturbing the centrifuged solution and analyzed spectrophotometrically by measuring the maximum absorbance at the wavelength, λ_{max}, of 582 nm. The experiments were carried out at three different temperatures (30, 40, and 50 °C). The amount of CV adsorbed on MCM-41 at equilibrium was obtained using the following equation,

$$q_e = \frac{(C_0 - C_e) \times V}{m}$$

where, q_e is the amount of dye adsorbed at equilibrium (mol g^{-1}), V is the volume of the solution (dm^3), m is the mass of the adsorbent (g), C_0 and C_e are the initial and equilibrium concentrations of the dye, respectively, computed from the calibration curve.

2.5 Kinetic studies

The influence of contact time on the amount of dye adsorbed were investigated at one fixed initial dye concentration (6.13×10^{-5}) by adding 50 ml of dye solution to 0.02 g of MCM-41. The mixture was shaken as a function of time in an incubator shaker at 100 rpm for three different temperatures. At various time intervals, samples were taken and the concentration was measured. The amount of CV adsorbed q_t at time t was determined by the following equation,

$$q_t = \frac{(C_0 - C_t) \times V}{m}$$

where, q_t is the amount of dye adsorbed at time t (mol g^{-1}), V is the volume of the solution (dm^3), m is the mass of the adsorbent (g), C_0 and C_t are the concentrations of the dye at initial ($t = 0$) and at time t, respectively.

The influence of pH on dye removal was carried out by performing the adsorption experiments in the pH range between 2 and 11 for three different temperatures (30, 40 and 50 °C). The pH of the solution was adjusted by adding a few drops of NaOH or HCl to reach the desired value, before shaking.

3 Result and discussions

3.1 Characterization of MCM-41 adsorbent

Thermo gravimetric (TG) analyses of the as-synthesized and calcined MCM-41 samples are shown in Fig. 1. The as-synthesized MCM-41 sample shows the weight loss in three distinct regions. The removal of water molecules physisorbed on the external surface of the materials causes the first region of weight loss (28%) between 50 and 100 °C. The second region of weight loss (7%) between 100 and 220 °C is attributed to the decomposition of the surfactant. The third region of weight loss (24%) between 220 and 550 °C is due to the combustion of the residual surfactant and loss of water that is generated from the condensation of adjacent silanol groups. The calcined MCM-41 shows two regions of weight loss (18%) and it is observed that only about 3% of weight loss after 120 °C, which shows that the surfactant is completely removed from the calcined MCM-41. Sulfated MCM-41 shows only 4% weight loss due to removal of physisorbed water molecule. The H_2SO_4 is completely decomposed at 550 °C, and it may be existed in the form of SO_4^{2-} (Haihong et al. 2006).

Figure 2 depicts the XRD patterns of the MCM-41 samples. Only one low-angle peak for d_{100} plane corresponding to the mesophase is observed in all the samples at 2θ value of 1.4 °, which is the characteristic of the long range hexagonal structure of MCM-41. This low value of 2θ is mainly due to the length of the carbon chain (C_{19}) used for synthesis of MCM-41 (Lin et al. 1997; Kaftan et al. 2005). There is no considerable change in the peak position and the intensity of the XRD peaks shows that the structure of sulfated MCM-41 is still mesoporous and similar to that of MCM-41. The textural properties of the MCM-41 samples are reported in Table 1.

The nitrogen adsorption/desorption isotherms and pore size distribution of the MCM-41 samples are shown in Fig. 3(a) and (b), respectively. The isotherms obtained for the as-synthesized MCM-41 shows a linear increase in the adsorbed volume with increase in the relative pressure up to 0.90. The MCM-41 calcined at 550 °C shows three distinct regions of N_2 adsorption isotherms. A linear increase in the adsorbed volume at low relative pressures ($P/P_0 \sim 0.28$), may be attributed to a monolayer-multilayer adsorption on the pore walls. At relative pressures between 0.28 and 0.42, a steeper increase of the adsorbed volume is observed. This is mainly due to capillary condensation of N_2 in the pore channels. A very little linear increase at higher relative pressures between 0.40 and 0.99 shows the multilayer adsorption on the outer surface. The sulfated MCM-41 follows the same pattern of the calcined MCM-41. The pore size distribution calculated through BJH method using desorption isotherm indicates that the synthesized MCM-41 samples containing only mesopores not micropores. All the MCM-41 samples maintain the same pattern of pore size distribution which is shown in Fig. 3(b). However, the total distribution is not available due to instrumental limitations to measure pore size below 3 nm (Saha and Ghoshal 2007). The BET surface area and pore volume of the calcined MCM-41 is found to be 1059 $m^2\,g^{-1}$ and 0.8905 ml g^{-1}, respectively. For the sulfated MCM-41, a decrease in surface area (938 $m^2\,g^{-1}$) is accompanied by a small decrease in pore volume and increase in average pore diameter. It is evident that sulfate plays a significant role in determining the structural char-

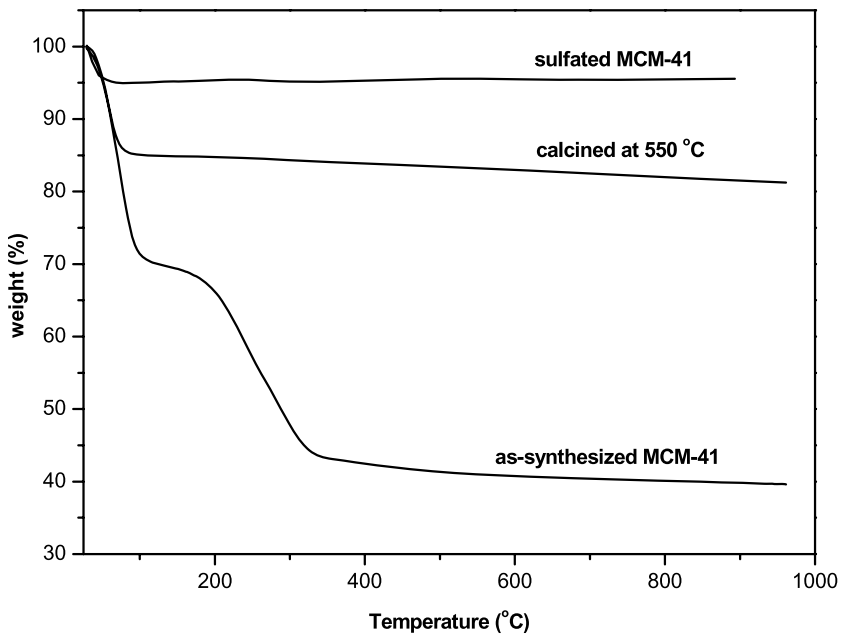

Fig. 1 Thermogravimetric curves of MCM-41 samples

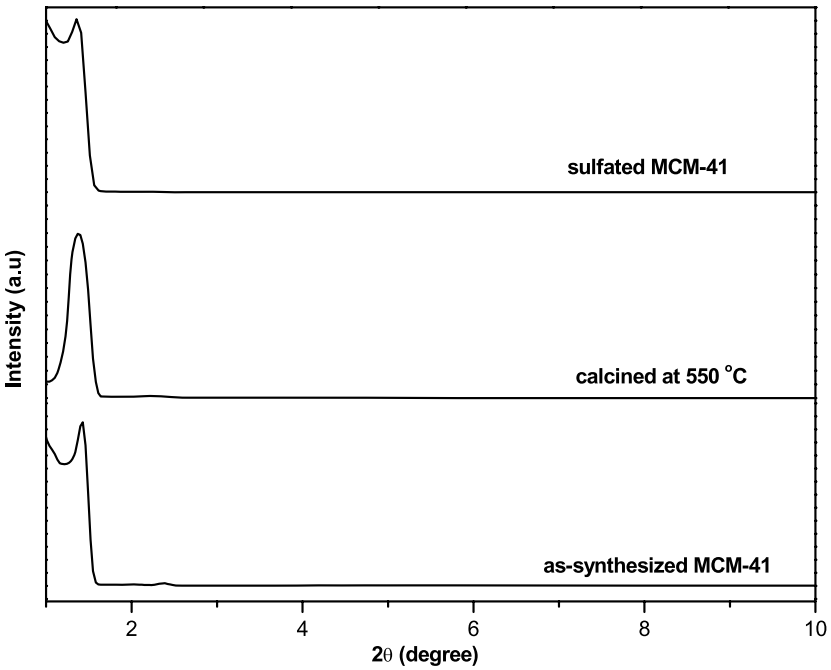

Fig. 2 XRD patterns of MCM-41 samples

Table 1 Textural properties of MCM-41 samples

Sample	X-ray diffraction			N_2 adsorption		
	d_{100} Spacing (nm)	Unit Cell Parameter[a] a_0 (nm)	Wall Thickness[b] (nm)	BET Surface Area ($m^2\ g^{-1}$)	Mesopore volume ($ml\ g^{-1}$)	Average Pore Diameter[c] D_p (nm)
As-synthesized	6.28	7.26	3.570	48.78	0.0450	3.690
Calcined MCM-41	6.40	7.39	4.028	1059.33	0.8905	3.362
Sulfated MCM-41	5.70	6.58	2.804	938.62	0.8865	3.778

[a]Unit Cell Parameter $= a_0 = 2 \times d_{100}/\sqrt{3}$ Where d_{100} is the d-spacing of (100) reflection

[b]Wall Thickness $= a_0 - D_p$

[c]Average Pore Diameter $D_p = 4V_{mes}/S_{BET}$. Where V_{mes} is the Mesopore volume and S_{BET} is the BET surface area

acteristics of MCM-41. After treating with H_2SO_4, the sulfate group may be converted into the polynuclear complex sulfates, possibly of $S_2O_7^{2-}$ type and block the pore mouths causing decrease in surface area and pore volume (Morterra et al. 1991).

Figure 4 shows the FT-IR spectra of the MCM-41 samples. The as-synthesized sample shows two very sharp intense bands at 2923 and 2852 cm^{-1}, that are due to the C-H stretching of the hydrocarbon chain of the surfactant molecules. The corresponding bending vibration mode is observed at 1489 cm^{-1}. In the hydroxyl region (3600–3200 cm^{-1}), a broad band is seen around 3410 cm^{-1}, which is attributed to surface silanols and adsorbed water molecules. The absorption bands close to 1648 cm^{-1} is due to the bending vibration of adsorbed water molecules. The asymmetric stretching vibrations of Si-O-Si are observed by the absorption bands at 1067 and 1230 cm^{-1}. The band at 970 cm^{-1} is attributed to Si-OH vibrations. The absorption peaks around 460 to 795 cm^{-1} are mainly due to bending vibration of Si-O-Si bonds and the band at 794 cm^{-1} may also correspond to free silica (Ghiaci et al. 2007). All the bands belonging to the organic groups are disappeared for the calcined and sulfated MCM-41, which confirms the complete removal of the surfactants. The FTIR spectrum obtained matches with Haihong et al. (2006) and Parida and Rath (2006) FTIR spectrums.

3.2 Adsorption isotherms

Adsorption isotherm study is performed with the calcined and sulfated MCM-41. Equilibrium isotherms are very important in the design of any adsorption processes. Generally,

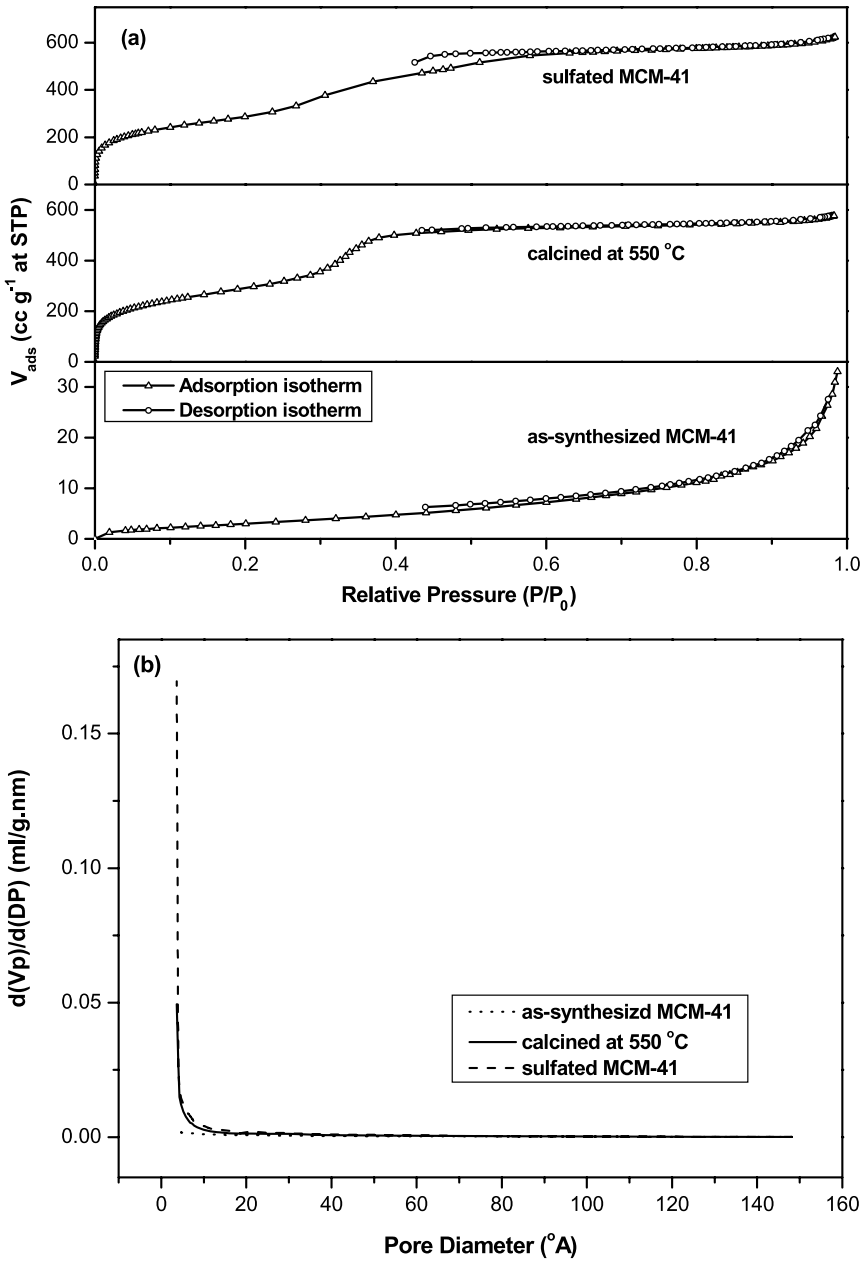

Fig. 3 N_2 adsorption/desorption isotherm (**a**) and pore size distribution (**b**) of MCM-41 samples

the adsorption isotherms with a specific adsorbate are carried out to estimate the adsorption characteristics. The concentration variation method is used to calculate the adsorption characteristic of the adsorbent and the process. The adsorption isotherms of CV on calcined and sulfated MCM-41 are measured at three different temperatures. The results are fitted with three important isotherm models such as Langmuir, Freundlich and Redlich-Peterson. The models are fitted with nonlinear expression without linearization because linearization leads to an error (high or low correlation coefficient) value of correlation coefficients (R^2), depending on in which form it is linearized. So it is difficult to predict the actual isotherm. Nonlinear method is the best way to get the actual isotherm parameters (Crini and Badot 2008; Vasanth Kumar 2006).

The Langmuir adsorption is based on the assumption of monolayer adsorption on a structurally homogeneous adsorbent, where all the sorption sites are identical and energetically equivalent. Where in, the adsorption occurs at specific homogeneous sites within the adsorbent and once a dye molecule occupies a site, no further adsorption can take place at that site. The intermolecular forces decrease rapidly with distance, and consequently the existence of monolayer coverage of the adsorbate at the outer surface of the adsor-

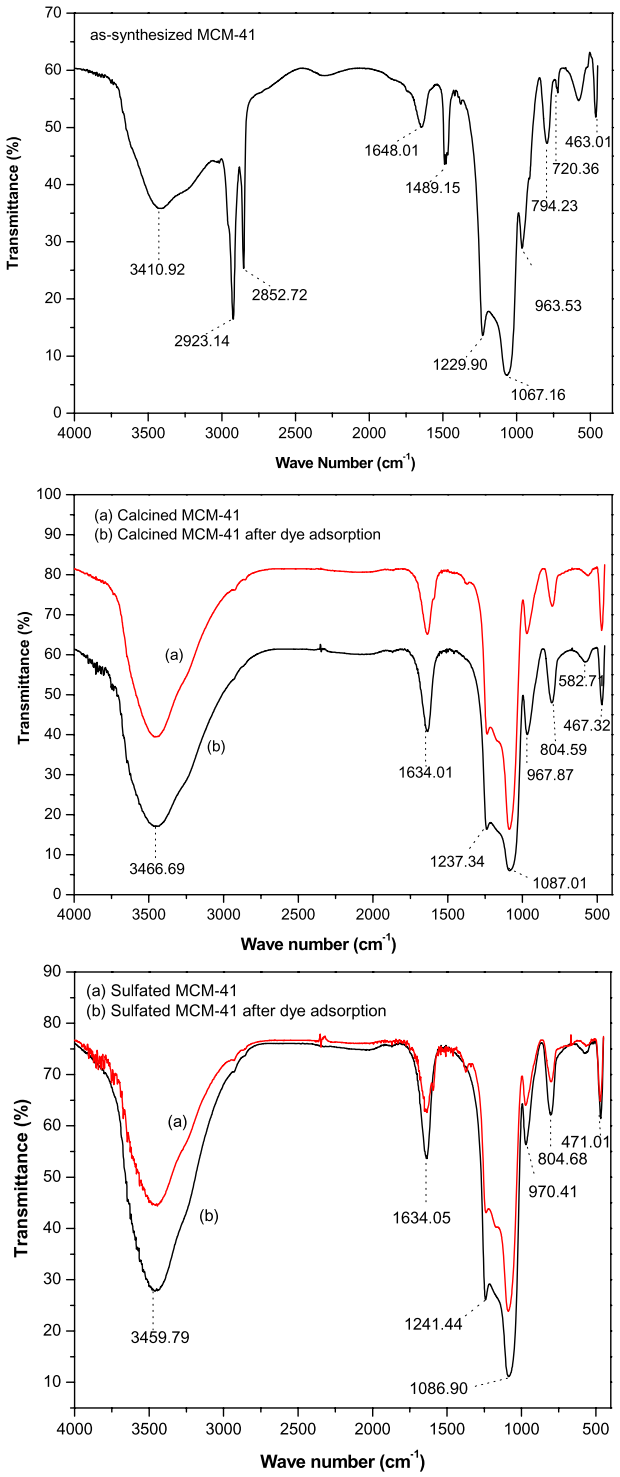

Fig. 4 FTIR Spectra of MCM-41 samples

bent could be predicted. The homogeneous Langmuir adsorption isotherm is represented by the following equation (Langmuir 1915).

$$q_e = \frac{Q_{\max} K_L C_e}{(1 + K_L C_e)}$$

where, q_e is the adsorbed amount of the dye at equilibrium (mol g^{-1}), C_e is the equilibrium concentration of the dye in solution (mol dm^{-3}), $Q_{\max}$ is the maximum adsorption capacity (mol g^{-1}) and K_L is the constant related to the free energy of adsorption (dm^3 mol^{-1}).

The Freundlich adsorption isotherm is one of the most widely used empirical equation, which fits with the experimental data over a wide range of concentrations. This is based on the assumption that the adsorption surface is heterogeneous and exponential distribution of active sites. It also assumes that an unlimited number of unreacted sites are available. The heterogeneous Freundlich adsorption isotherm is represented by the following equation (Freundlich 1907),

$$q_e = K_F C_e^{1/n}$$

where, K_F is the Freundlich isotherm constant (mol/g$(dm^3/mol)^{1/n}$), which is an indicative of the extent of adsorption (i.e., adsorption capacity) and $1/n$ is the adsorption intensity (dimensionless). The exponent $1/n$ is usually less than 1.0 because sites with the highest binding energies are utilized first, followed by weaker sites, and so on.

The three parameter Redlich-Peterson isotherm model combines the features of both Freundlich and Langmuir isotherm equations. Its adsorption mechanism does not obey ideal monolayer adsorption, but an impure one i.e., it approaches the Freundlich model at high concentrations and at low concentration, it approaches to Langmuir equation. The Redlich-Peterson isotherm can be described by the equation (Redlich and Peterson 1959),

$$q_e = \frac{K_{RP} C_e}{1 + \alpha C_e^g}$$

where, K_{RP} and α are the Redlich-Peterson constants and g is the exponent which lies between 0 and 1. For $g = 1$, the above equation reduces to Langmuir form. This model can describe the adsorption process over a wide range of concentrations.

All the three isotherm models are fitted with the experimental data and are shown in Fig. 5. The corresponding typical parameter values are given in Table 2. It can be observed from the Table 2, that the maximum adsorption capacity decreases with increase in temperature for both calcined and sulfated MCM-41. The high adsorption capacity of sulfated MCM-41 is due to the acid sites generated by the sulfate groups. Based on the correlation coefficients (R^2 value) it is found that the Redlich-Peterson isotherm is the most-suitable isotherm for the experimental data and followed by the Langmuir and then Freundlich isotherm. With

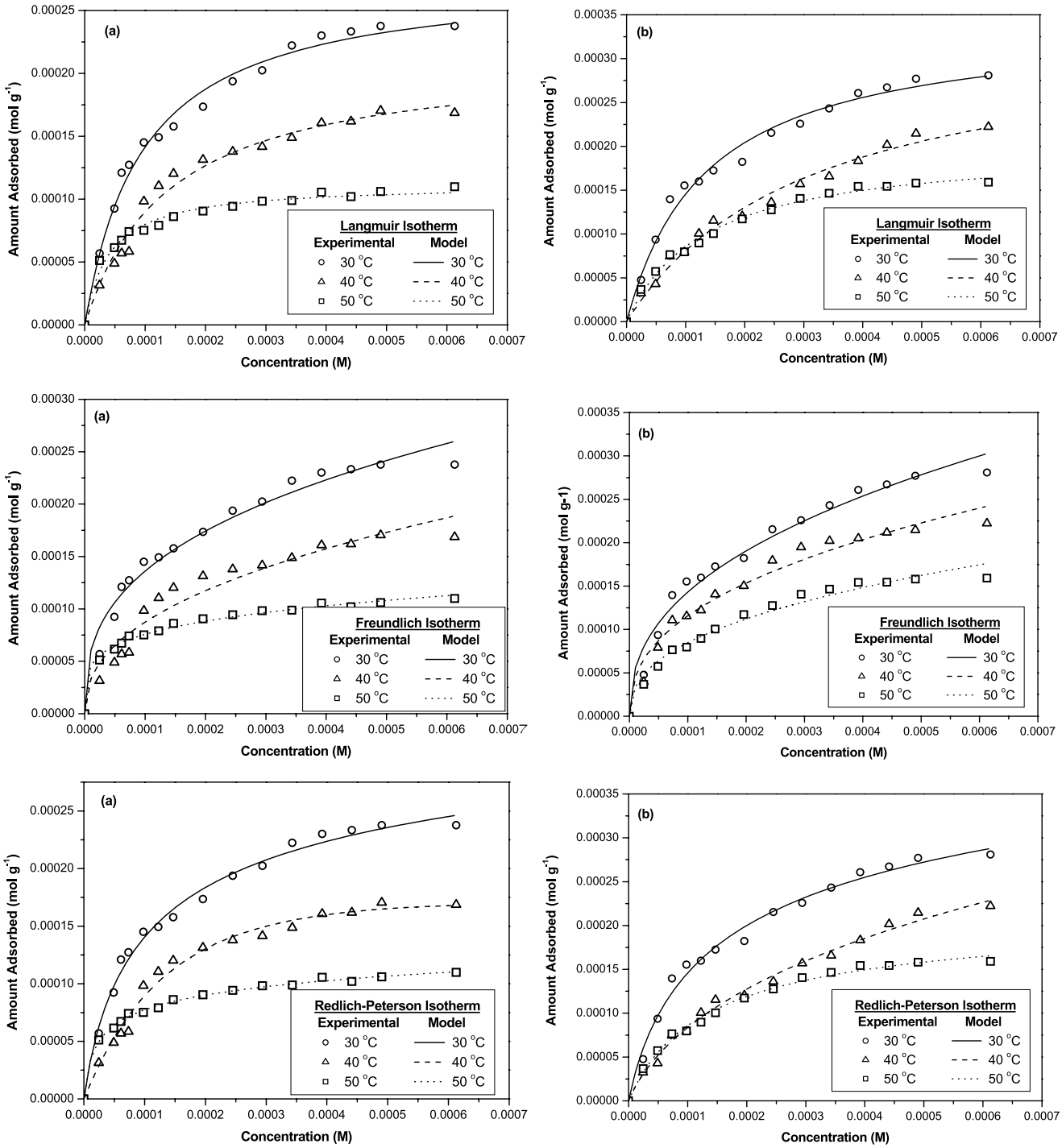

Fig. 5 Adsorption isotherm models of CV on calcined MCM-41 (**a**) and sulfated MCM-41 (**b**) at different temperatures

an increase in the temperature, the maximum adsorption capacity decreases and the Langmuir constant increases, respectively. A high value of K_L indicates higher affinity, but the obtained results indicates that the Langmuir model is not appropriate for the description of adsorption of CV on both calcined and sulfated MCM-41. The lower values of K_F at higher temperatures indicates that the CV posses higher adsorption capacity at lower temperatures and the value $1/n$ is less than 1 for all the temperature indicates a favourable adsorption of CV on the MCM-41. The adsorption capacity for CV tends to decrease with increase in the temperature and shows that the dye molecules may not have sufficient energy to undergo an interaction with active sites at the surface. The value of g lies between 0 and 1 also indicates a favourable

Table 2 Parameters of adsorption isotherms of CV on calcined MCM-41 and sulfated MCM-41 at different temperatures

Adsorbent	Isotherm Model	Parameters	Temperature (°C)		
			30	40	50
Calcined MCM-41	Langmuir Model	Q_{max} (mol g^{-1})	2.8×10^{-4}	2.1×10^{-4}	1.1×10^{-4}
		K_L (dm^3 mol^{-1})	1.039×10^4	1.234×10^4	2.509×10^4
		R^2	0.989	0.995	0.984
	Freundlich Model	K_F (mol g^{-1} (dm^3 mol^{-1})$^{1/n}$)	3.63×10^{-3}	2.26×10^{-3}	5.8×10^{-4}
		$1/n$	0.356	0.327	0.221
		R^2	0.976	0.978	0.981
	Redlich-Peterson Model	K_{RP} (mol g^{-1})	3.75	3.18	6.72
		α ((dm^3 mol^{-1})^g)	0.5896×10^4	0.8210×10^4	2.0444×10^4
		g	0.887	0.917	0.856
		R^2	0.992	0.996	0.996
Sulfated MCM-41	Langmuir Model	Q_{max} (mol g^{-1})	3.4×10^{-4}	2.7×10^{-4}	2.0×10^{-4}
		K_L (dm^3 mol^{-1})	7.411×10^3	7.551×10^3	7.493×10^3
		R^2	0.988	0.991	0.993
	Freundlich Model	K_F (mol g^{-1} (dm^3 mol^{-1})$^{1/n}$)	6.44×10^{-3}	4.90×10^{-3}	3.48×10^{-3}
		$1/n$	0.413	0.406	0.404
		R^2	0.977	0.972	0.978
	Redlich-Peterson Model	K_{RP} (mol g^{-1})	3.38	2.24	1.64
		α ((dm^3 mol^{-1})^g)	3.439×10^3	5.769×10^3	5.612×10^3
		g	0.854	0.951	0.948
		R^2	0.990	0.992	0.993

adsorption. The value of g is found to be greater than 0.86 for all the temperature and the model shows that the adsorption is very close to Langmuir model (for Langmuir model $g = 1$). Although the Redlich-Peterson and Langmuir model gives a better fitting result than the Freundlich model, the Q_{max} and K_L values on temperature for CV dye, violates the thermodynamic consistency (discussed later). The increase in K_L with increase in temperature indicates that the adsorption process is endothermic in nature, which contradicts with the result as shown in Fig. 5. From the thermodynamic relation, it is observed that the Redlich-Peterson and Langmuir model are not appropriate model for the description of the CV dye on calcined and sulfated MCM-41. The sulfated MCM-41 shows a maximum adsorption capacity of 3.4×10^{-4} mol g^{-1} than the calcined MCM-41 (2.8×10^{-4} mol g^{-1}). The maximum adsorption capacity of CV dye on calcined and sulfated MCM-41 in this present work, is comparable to the work reported earlier which is shown in Table 3. The difference in adsorption capacity is due to the various synthesis procedures followed by the researcher and surface chemistry of the MCM-41.

3.3 Thermodynamic parameters

Thermodynamic parameters for the adsorption of CV on calcined and sulfated MCM-41 is evaluated by the equilibrium experimental data obtained at different temperatures. Free energy, enthalpy and entropy are considered to be the key factors in the design of adsorption process. The change in Gibbs free energy (ΔG^0) of the adsorption process is related to the equilibrium constant by the following equation,

$$\Delta G^0 = -RT \ln K$$

The thermodynamic parameters, change in enthalpy (ΔH^0) and change in entropy (ΔS^0) are related to the Gibbs free energy (ΔG^0), are calculated based on the adsorption isotherms by the following equations,

$$\Delta H^0 = -R \left(\frac{T_2 T_1}{T_2 - T_1} \right) \ln \frac{K_2}{K_1}$$

$$\Delta S^0 = \frac{\Delta G^0 - \Delta H^0}{T}$$

where, K_1 and K_2 are the Langmuir constants at $T_1 = 30\,^\circ$C and $T_2 = 50\,^\circ$C, respectively. The ΔG^0 values for

Table 3 Adsorption capacity of CV on various adsorbents

Adsorbent	Adsorption Capacity (mol g^{-1})	Reference
Activated Carbon Sludges	6.45×10^{-4}	Otero et al. (2003)
Pyrolysed sludges	4.52×10^{-4}	Otero et al. (2003)
Jute fiber Carbon	0.68×10^{-4}	Porkodi and Vasanth Kumar (2007)
Sulfuric acid activated Carbon from coconut male flowers	2.10×10^{-4}	Senthilkumaar et al. (2006)
Phosphoric acid activated Carbon from coconut male flowers	1.48×10^{-4}	Senthilkumaar et al. (2006)
Charred saw dust	4.79×10^{-4}	Chakraborty et al. (2005)
Palygorskite	1.24×10^{-4}	Al-Futaisi et al. (2007)
Activated Carbon from rice husk	1.67×10^{-4}	Graham et al. (2001)
Raw sepiolite	1.80×10^{-4}	Eren and Afsin (2007)
Raw Bentonite	3.50×10^{-4}	Eren and Afsin (2008)
Natural Zeolite	3.5×10^{-5}	Li et al. (2006)
MCM-41	5.8×10^{-4}	Lee et al. (2007)
MCM-22	1.20×10^{-4}	Wang et al. (2006)
Calcined MCM -41	2.80×10^{-4}	Present Work
Sulfated MCM-41	3.40×10^{-4}	Present Work

the adsorption of CV on calcined and sulfated MCM-41 are found to be −23.30 (−24.52 and −27.21 KJ mol^{-1}) and −22.45 KJ mol^{-1} (−23.24 and −23.96 KJ mol^{-1}) at 30 °C (40 °C and 50 °C), respectively. The ΔH^0 and ΔS^0 values for the adsorption of CV on calcined and sulfated MCM-41 are found to be −35.87 and −0.4477 KJ mol^{-1} and −41.49 and 72.61 J mol^{-1} K^{-1} , respectively. The negative values of ΔG^0 indicates that the adsorption of CV on both MCM-41 are thermodynamically feasible and spontaneous at room temperature. The ΔG^0 values obtained are in the middle of physical adsorption and chemisorption (Crini and Badot 2008). The negative values of ΔH^0 confirms that the adsorption is exothermic in nature. The high values of ΔH^0 for the calcined MCM-41 suggests that the interactions between CV and the surface hydroxyl groups are very strong compared with sulfated MCM-41 (Juang et al. 2006). The calcined MCM-41 shows a negative ΔS^0 value suggests that there is no significant changes occurred in the internal structure of the adsorbent.The positive value of ΔS^0 for sulfated MCM-41 indicates an increased randomness at the solid/solution interface with some structural changes in the adsorbate and adsorbent and an affinity of the MCM-41 towards CV. Also, positive ΔS^0 value corresponds to an increase in the degree of freedom of the adsorbed species (Chakraborty et al. 2005).

3.4 Effect of pH

The pH of the solution affects the surface charge of the adsorbent and the degree of ionization of the materials present in the solution. It affects the structural stability and its color intensity and hence it is an important controlling parameter in adsorption process. The percentage removal of CV dye using calcined and sulfated MCM-41 over a pH range of 2 to 11 with a solution of initial concentration 1.23×10^{-4} M is shown in Fig. 6. Both the MCM-41 follows the same trend and the percentage removal of CV dye is more or less equal. The percentage removal of CV is increased with increase in the pH from 4 to 11, with the maximum removal (>98%) at pH 11. The increased adsorption at higher pH is mainly due to enhanced association of the dye cations. It is related to the electrostatic attraction force of the dye compound with MCM-41 surface that is likely to be raised, when the pH increases. An increase of pH of the solution decreases the charge density, so the electrostatic repulsion between the positively charged dye and the surface of the adsorbent is lowered, which results in an increase in the extent of adsorption of CV. The minimum removal of CV is found at pH 4 and is probably due to the presence of excess H^+ ions competing with the cation groups on the dye for adsorption sites. Increase in the CV removal at pH 2 may be due to the dissociation of the dye. Similar observations were previously reported for the adsorption of CV on MCM-41 (Lee et al. 2007).

3.5 Kinetic study

The factors affecting the reaction rates for the adsorption of CV on calcined and sulfated MCM-41 are studied through adsorption kinetic experiments. Adsorption kinetics also explains how fast or slow the chemical reaction occurs, which

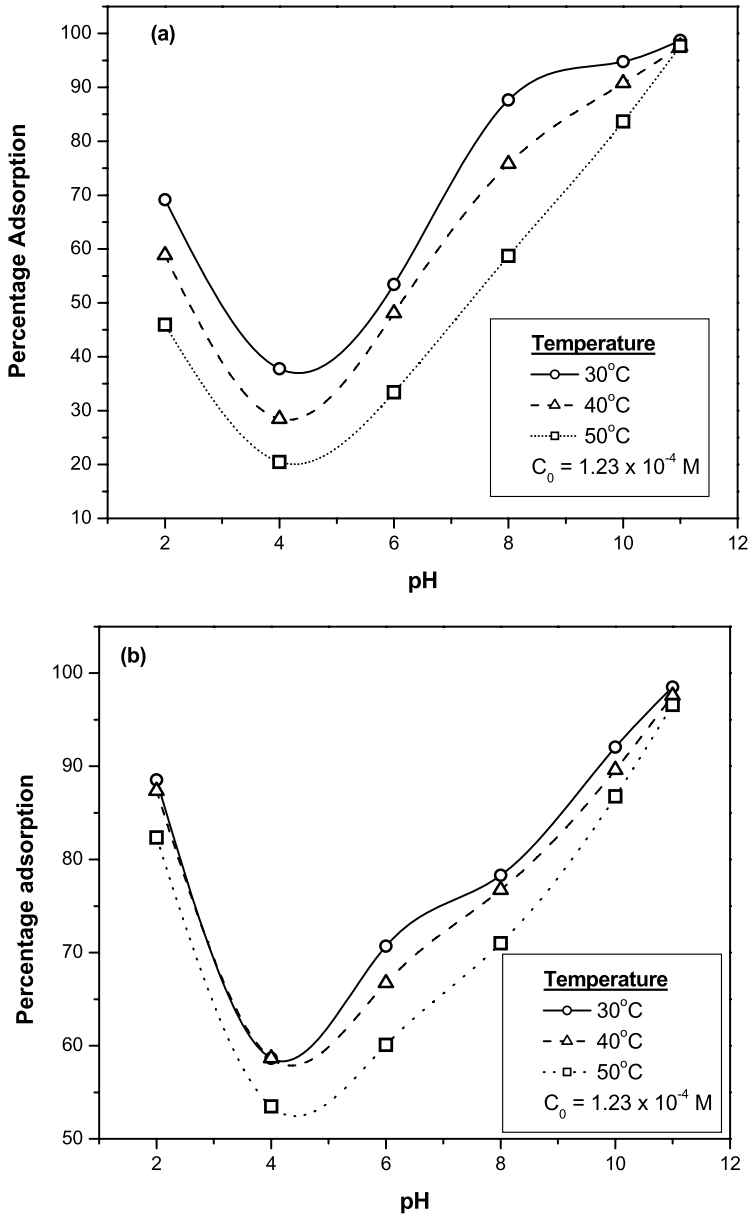

Fig. 6 pH effect of CV adsorption on calcined MCM-41 (**a**) and sulfated MCM-41 (**b**) at different temperatures

should be very useful in the selection of the adsorbent material. Pseudo-first-order kinetic model (Lagregren 1898), pseudo-second-order kinetic model (Ho and McKay 1999) and intraparticle diffusion model (Weber and Morris 1963) are investigated for the adsorption of CV on calcined and sulfated MCM-41. The pseudo-first order rate expression is generally described by the following equation,

$$\frac{dq_t}{dt} = k_1(q_e - q_t)$$

where, k_1 is the pseudo-first-order rate constant (min^{-1}), q_e and q_t are the amount of dye adsorbed at equilibrium (mol g^{-1}) and at time t (mol g^{-1}), respectively. The above equation can be transformed into nonlinear forms to predict the adsorption equilibrium.

$$q_t = q_e(1 - e^{-k_1 t})$$

The pseudo-second-order rate equation can be explained by the following equation,

$$\frac{dq_t}{dt} = k_2(q_e - q_t)^2$$

where, k_2 is the rate constant of pseudo-second-order adsorption mechanism ($\text{g mol}^{-1}\,\text{min}^{-1}$). Integrating and ap-

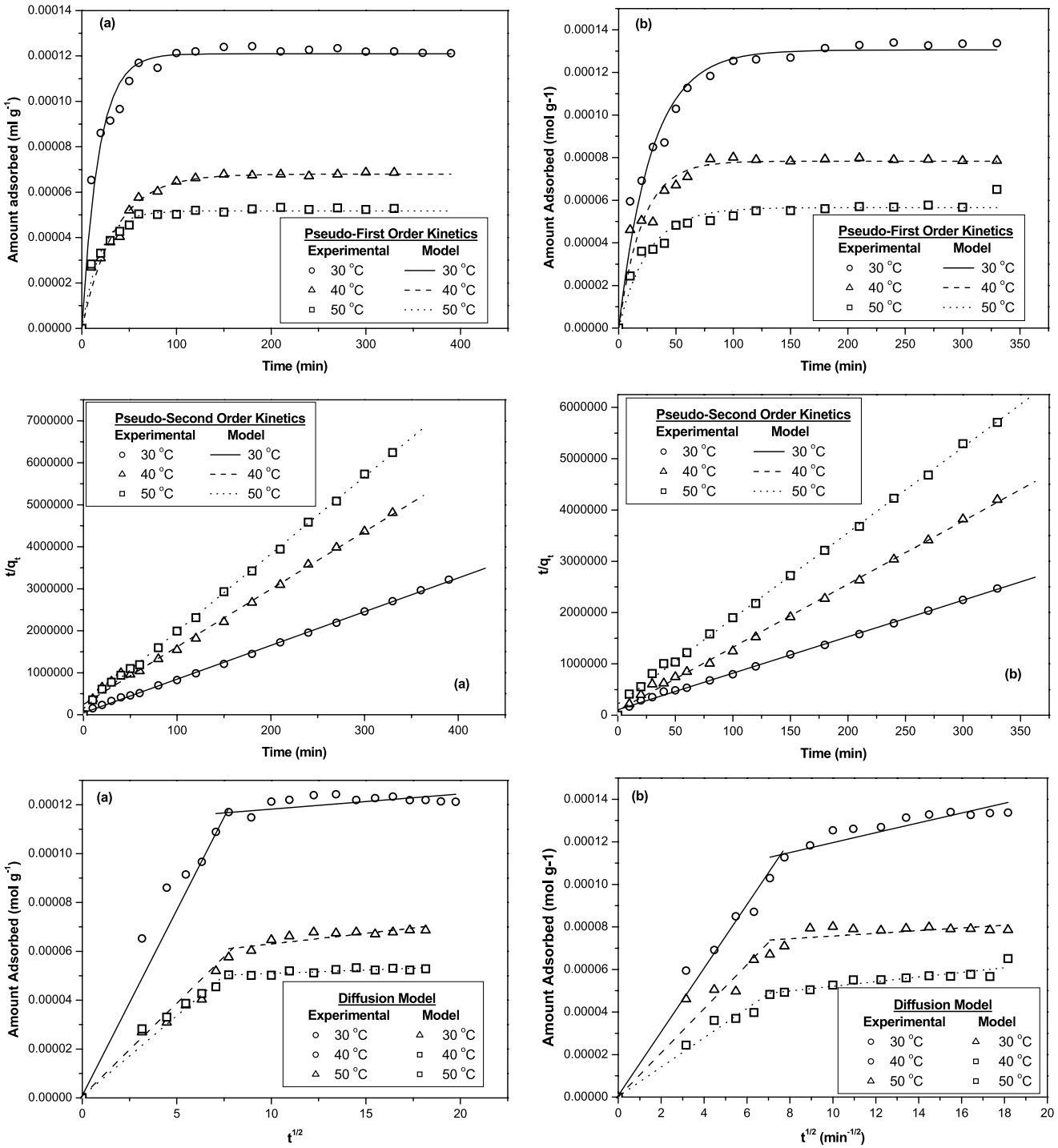

Fig. 7 Kinetic models of CV on calcined MCM-41 (**a**) and sulfated MCM-41 (**b**)

plying boundary conditions $t = 0$ and $q_t = 0$ to $t = t$ and $q_t = q_e$ and rearranging, it becomes

$$\frac{t}{q_t} = \frac{1}{k_2 q_e^2} + \frac{1}{q_e} t$$

Figure 7 presents the adsorption kinetics of CV on calcined and sulfated MCM-41. From Table 2, it is clear that the regression coefficients of second-order kinetics are greater than the first-order kinetic model for the adsorption of CV dye on both calcined and sulfated MCM-41. The above result suggests that the rate-limiting step may be

Table 4 Parameters of kinetic models of CV adsorption on MCM-41 at different temperatures

Calcined MCM-41								
Temperature (°C)	Pseudo-first-order kinetic model			Pseudo-second-order kinetic model			Diffusion model	
	k_1 (min^{-1})	q_e (mol g^{-1})	R^2	k_2 (g mol^{-1} min^{-1})	q_e (mol g^{-1})	R^2	K_d	R^2
30	0.0561	1.2×10^{-4}	0.972	1.46×10^{3}	1.24×10^{-4}	0.999	6.22×10^{-7}	0.396
40	0.0290	0.7×10^{-4}	0.977	0.721×10^{3}	0.73×10^{-4}	0.999	8.69×10^{-7}	0.708
50	0.0527	0.5×10^{-4}	0.973	2.37×10^{3}	0.54×10^{-4}	0.999	2.81×10^{-7}	0.718
Sulfated MCM-41								
Temperature (°C)	Pseudo-first-order kinetic model			Pseudo-second-order kinetic model			Diffusion model	
	k_1 (min^{-1})	q_e (mol g^{-1})	R^2	k_2 (g mol^{-1} min^{-1})	q_e (mol g^{-1})	R^2	K_d	R^2
30	0.0348	1.3×10^{-4}	0.968	0.476×10^{3}	1.41×10^{-4}	0.998	2.32×10^{-6}	0.794
40	0.0487	0.8×10^{-4}	0.940	1.651×10^{3}	0.81×10^{-4}	0.998	0.64×10^{-7}	0.353
50	0.0390	0.6×10^{-4}	0.951	0.968×10^{3}	0.62×10^{-4}	0.992	1.09×10^{-6}	0.834

chemisorption and the rate equation follows second-order kinetics.

To identify the steps involved during adsorption process, a diffusion model is investigated for CV adsorption on calcined and sulfated MCM-41. The diffusion model involves two steps, which suggests that the adsorption process proceeds by surface sorption and intraparticle diffusion. The diffusion model expressed by the following equation

$$q_t = k_d t^{1/2} + c$$

where, k_d is the diffusion coefficient and c is the intercept indicating the boundary-layer surface sorption. Generally, the initial curved portion appears in the adsorption is due to the boundary-layer effect and the second linear portion of the plot is obtained because of intraparticle or pore diffusion (Lee et al. 2007). If the regression is linear and passes through the origin, then intraparticle diffusion is the rate-limiting step. The plot of q_e versus $t^{1/2}$ doesn't pass through the origin suggesting that adsorption involved intraparticle diffusion. It can be seen from the Table 4, the k_d values decreased with increase in temperature shows that the mobility of CV dye molecules onto the MCM-41 decreases with increase in temperature.

3.6 Proposed adsorption mechanism

MCM-41 surface is constructed by OH groups and oxygen bridges, which act as adsorption sites. In the adsorption processes, it is very important to know the characteristics of these different adsorption sites. Generally, OH groups acts as centers for adsorption through forming hydrogen bonds with the adsorbate and could be divided into: (i) isolated free silanol (–SiOH), (ii) geminal free silanol (–$Si(OH)_2$), and (iii) vicinal or bridged or OH groups bound through the hydrogen bond (Khraisheh et al. 2005). In addition, MCM-41 consists of siloxane groups or –Si–O–Si– bridges with oxygen atoms on the surface.

FTIR technique is an interesting application for studying the interaction between an adsorbate and the active groups on the surface of adsorbent. Consequently, the adsorption of CV dye onto calcined and sulfated MCM-41 is investigated in order to get some insight into the nature of the mechanism of adsorbent-adsorbate interaction. Figure 4 shows FTIR spectra of calcined and sulfated MCM-41 before and after CV dye adsorption. Based on the result obtained from FTIR and thermodynamic parameter analysis, two mechanisms are proposed for the adsorption of CV dye on calcined and sulfated MCM-41. First mechanism is adsorption by n-π interaction and the second mechanism is adsorption by an electrostatic attraction between the dye and the surface of the adsorbents. The adsorption of CV dye on calcined MCM-41 is proposed by Scheme 1.

As seen from Fig. 4, calcination process lead to the formation of surface siloxane groups or –Si–O–Si– bridges, which probably act as an active site for dye adsorption. During calcination, the band shifts from 3410 to 3466 cm^{-1} and the intensity is more than the as-synthesized MCM-41 that indicates the formation of new surface hydroxyl groups via H bonds. After dye adsorption, there is a shift in the band position and the decreased intensity of the peaks indicates a decrease in the surface hydroxyl group due to dye adsorption. No new bands have been found after dye adsorption indicating that the dye molecules are adsorbed only on the pores of calcined MCM-41. It implies that the adsorption on calcined MCM-41 may be due to electrostatic interaction. Since electrostatic interactions are strong interaction,

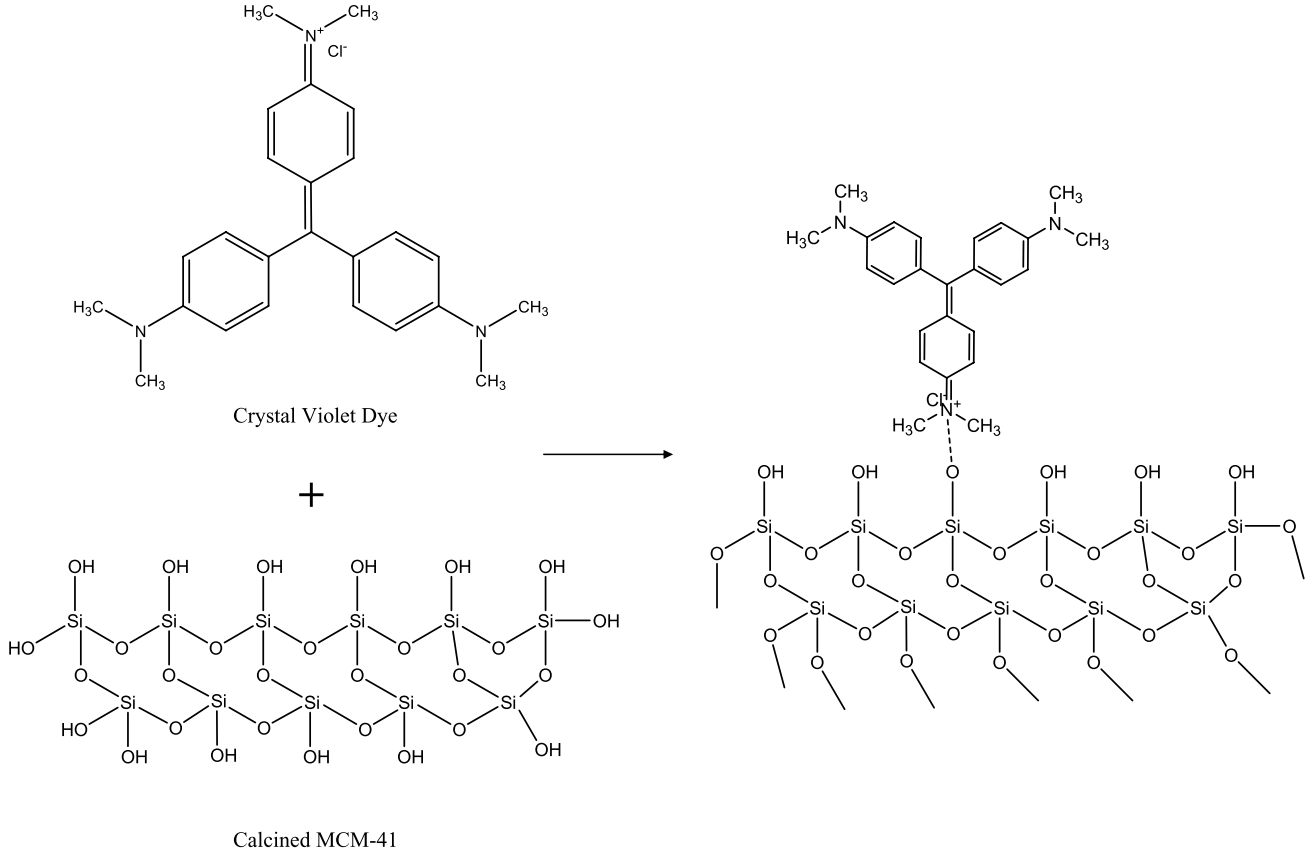

Scheme 1 Proposed adsorption mechanism of crystal violet dye on calcined MCM-41

the ΔG^0 value of calcined MCM-41 is higher than the sulfated MCM-41 for all the studied temperatures. The higher negative values of ΔH^0 also shows that the interaction of adsorbent-adsorbate is strong due to electrostatic interaction. The negative value of change in entropy indicates no randomness and the interaction is only due to structural OH on the surface of the adsorbent and the cation dye molecule.

Adsorption of CV dye on sulfated MCM-41 may be due to the contribution of n-π interaction as represented in Scheme 2. Generally, the absorption of asymmetric stretching frequency of S=O bonds is commonly found in the range of 1360–1410 cm^{-1}. The absorption band of S=O band is not clearly visible in the sulfated MCM-41 (see Fig. 4). However, it is clearly visible (bands at 1340 and 1362 cm^{-1}) after adsorption of dye. The more intense band at 1340 and 1362 cm^{-1} suggests that S=O contributes for the dye adsorption. In case of sulfated MCM-41, there is a decrease in the surface hydroxyl group as well as the formation of new band at 1362 cm^{-1} indicates that the S=O also contributes for the adsorption of CV dye. The dye molecule sits flat on the surface during n-π interaction which covers/buries some of the hydroxyl groups. Due to this constraint environment of the OH group, it stretches more, which is identified by the shoulders on the OH band at 3444 cm^{-1}. An increased amount of dye adsorbed on sulfated MCM-41 may be due to n-π interaction as well as electrostatic interaction of the dye molecule on sulfated MCM-41 surface. A small value of ΔH^0 (−0.45, close to zero) indicates that the n-π interaction dominates over the electrostatic interaction. In n-π interactions, the dye molecule sits flat to the surface of the adsorbent surface. Since the n-π interaction is weak in nature, the dye molecule slides easily over the surface of the sulfated MCM-41. Because of this reason, a positive value of ΔS^0 is obtained which suggests that an increase in the degrees of freedom of the adsorbed species. One can see that there is no significant change in ΔG^0 value for the calcined and sulfated MCM-41. Because of this reason there is not much increment in the adsorption of dye on the sulfated MCM-41.

4 Conclusions

MCM-41 has been successfully synthesized at room temperature by the classical synthesis procedure. The surface of the MCM-41 is modified with sulfuric acid by wetness impregnation method. The MCM-41 samples are characterized with physico-chemical technique. The TGA result confirms

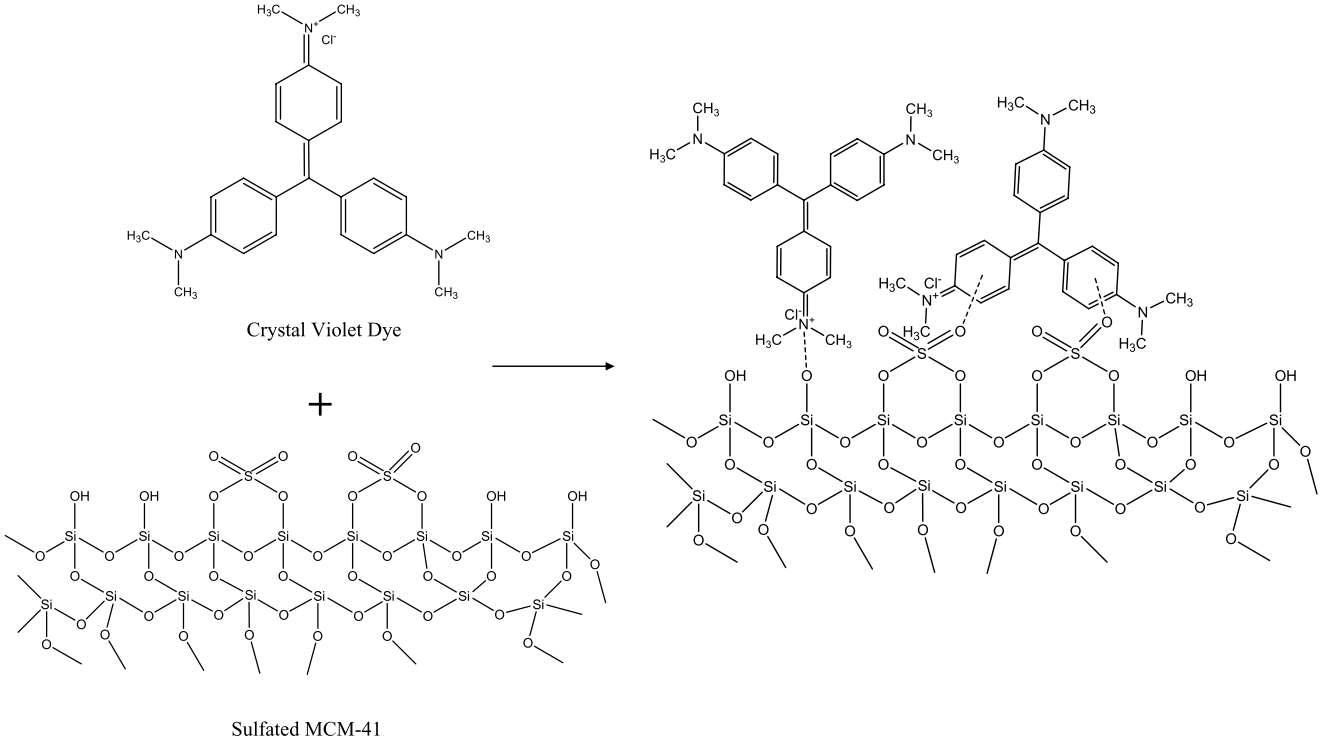

Scheme 2 Proposed adsorption mechanism of crystal violet dye on sulfated MCM-41

that the surfactant is completely removed from the calcined MCM-41 at 550 °C. There is no shift in the peak position of the XRD patterns for all MCM-41 samples and confirms that the structural stability is not affected by calcination and sulfation. Sulfated MCM-41 shows a maximum adsorption capacity compared to the calcined MCM-41. The adsorption capacity decreases with increase in temperature shows that the adsorption is exothermic in nature, which is also confirmed with the thermodynamic parameter studies. The removal efficiency of CV increases with increase in pH for both the MCM-41 adsorbent. It is observed that Freundlich isotherm is found to be more suitable and appropriate model to explain the adsorption isotherm of CV on MCM-41. The thermodynamic investigation shows that ΔG^0 and ΔH^0 are negative at all temperatures for both the adsorbents indicating that the adsorption is exothermic and spontaneous in nature. The results obtained from the kinetic study confirm the adsorption of CV follows pseudo-second order rate equation.

Acknowledgements The authors are thankful to the Centre for Nanotechnology, and Department of Chemistry, IIT Guwahati for helping in XRD and FTIR analysis, respectively.

References

Adak, A., Bandyopadhyay, M., Pal, A.: Removal of crystal violet dye from wastewater by surfactant-modified alumina. Sep. Purif. Technol. **44**, 139–144 (2005)

Al-Futaisi, A., Jamrah, A., Al-Hanai, R.: Aspects of cationic dye molecule adsorption to palygorskite. Desalination **214**, 327–342 (2007)

Aquino, J.M.F.B., Souza, C.D.R., Araujo, A.S.: Synthesis and characterization of sulfate-supported MCM-41 material. Int. J. Inorg. Mater. **3**, 467–470 (2001)

Chakraborty, S., De, S., DasGupta, S., Basu, J.K.: Adsorption study for the removal of a basic dye: experimental and modeling. Chemosphere **58**, 1079–1086 (2005)

Crini, G., Badot, P.M.: Application of chitosan, a natural aminopolysaccharide, for dye removal from aqueous solutions by adsorption processes using batch studies: A review of recent literature. Prog. Polym. Sci. **33**, 399–447 (2008)

Crini, G.: Non-conventional low-cost adsorbents for dye removal: A review. Bioresour. Technol. **97**, 1061–1085 (2006)

Eren, E., Afsin, B.: Investigation of a basic dye adsorption from aqueous solution onto raw and pre-treated sepiolite surfaces. Dyes Pigments **73**, 162–167 (2007)

Eren, E., Afsin, B.: Investigation of a basic dye adsorption from aqueous solution onto raw and pre-treated bentonite surfaces. Dyes Pigments **76**, 220–225 (2008)

Freundlich, H.: Uber die Adsorption in Losungen. J. Phys. Chem. **57**, 385–470 (1907)

Garg, V.K., Amita, M., Kumar, R., Gupta, R.: Basic dye (methylene blue) removal from simulated wastewater by adsorption using Indian rosewood sawdust: a timber industry waste. Dyes Pigments **63**, 243–250 (2004)

Ghiaci, M., Abbaspur, A., Kia, R., Belve, C., Trujillano, R., Rives, V., Vicente, M.A.: Vapor-phase alkylation of toluene by benzyl alcohol on H_3PO_4-modified MCM-41 mesoporous silicas. Catal. Commun. **8**, 49–56 (2007)

Graham, N., Chen, X.G., Jayaseelan, S.: The potential application of activated carbon from sewage sludge to organic dyes removal. Water Sci. Technol. **43**, 245–252 (2001)

Haihong, X., Daishi, G., Qizhong, J., Zifeng, M., Wanjun, L., Zheng, W.: Catalytic performance of sulfated silica MCM-41 for the cyclization of pseudoionone to ionones. Chin. J. Catal. **27**, 1080–1086 (2006)

Ho, Y.S., McKay, G.: Pseudo-second-order model for sorption processes. Process Biochem. **34**, 451–465 (1999)

Ho, Y., McKay, G., Yeung, K.L.: Selective adsorbents from ordered mesoporous silica. Langmuir **19**, 3019–3024 (2003)

Juang, L.C., Wang, C.C., Lee, C.K.: Adsorption of basic dyes onto MCM-41. Chemosphere **64**, 1920–1928 (2006)

Kaftan, O., Acikel, M., Eroglu, A.E., Shahwan, T., Artok, L., Ni, C.: Synthesis, characterization and application of a novel sorbent, glucamine-modified MCM-41, for the removal/preconcentration of boron from waters. Anal. Chim. Acta **47**, 31–41 (2005)

Khraisheh, M.A.M., Al-Ghouti, M.A., Allen, S.J., Ahmad, M.N.: Effect of OH and silanol groups in the removal of dyes from aqueous solution using diatomite. Water Res. **39**, 922–932 (2005)

Kumar, D., Schumacher, K., Hohenesche, C.F., Grun, M., Unger, K.K.: MCM-41, MCM-48 and related mesoporous adsorbents: their synthesis and characterization. Colloids Surf. A **187**, 109–116 (2001)

Lagregren, S.: About the theory of so-called adsorption of soluble substances. Kungl. Sven. Veten. Akad. Handl. **24**, 1–39 (1898)

Langmuir, I.: Chemical reactions at low pressures. J. Am. Chem. Soc. **27**, 1139–1143 (1915)

Lee, C.K., Liu, S.S., Juang, L.C., Wang, C.C., Lin, K.S., Lyu, M.D.: Application of MCM-41 for dyes removal from wastewater. J. Hazard. Mater. **147**, 997–1005 (2007)

Li, L., Wang, S., Zhu, Z.: Geopolymeric adsorbents from fly ash for dye removal from aqueous solution. J. Colloid Interface Sci. **300**, 52–59 (2006)

Lin, H.P., Cheng, S., Mou, C.Y.: Effect of delayed neutralization on the synthesis of mesoporous MCM-4 1 molecular sieves. Microporous Mater. **10**, 111–121 (1997)

Liu, C.H., Wu, J.S., Chiu, H.C., Suen, S.Y., Chu, K.H.: Removal of anionic reactive dyes from water using anion exchange membranes as adsorbers. Water Res. **41**, 1491–1500 (2007)

Morterra, C., Orio, L., Bolis, V., Ugliengo, P.: Bi-dimensional CO clusters at the surface of polycrystalline monoclinic ZrO. Mater. Chem. Phys. **29**, 457–466 (1991)

Namasivayam, C., Sumithra, S.: Removal of direct red 12B and methylene blue from water by adsorption onto Fe (III)/Cr (III) hydroxide, an industrial solid waste. J. Environ. Manag. **74**, 207–215 (2005)

Otero, M., Rozada, F., Calvo, L.F., Garci, A.I., Moran, A.: Elimination of organic water pollutants using adsorbents obtained from sewage sludge. Dyes Pigments **57**, 55–65 (2003)

Parida, M., Rath, D.: Studies on MCM-41: Effect of sulfate on nitration of phenol. J. Mol. Catal. A, Chem. **258**, 38–387 (2006)

Porkodi, K., Vasanth Kumar, K.: Equilibrium, kinetics and mechanism modeling and simulation of basic and acid dyes sorption onto jute fiber carbon: Eosin yellow, malachite green and crystal violet single component systems. J. Hazard. Mater. **143**, 311–327 (2007)

Redlich, O.J., Peterson, D.L.: A useful adsorption isotherm. J. Phys. Chem. **63**, 1024–1026 (1959)

Saha, B., Ghoshal, A.K.: Model-free kinetics analysis of decomposition of polypropylene over Al-MCM-41. Thermochim. Acta **460**, 77–84 (2007)

Senthilkumaar, S., Kalaamani, P., Subburaam, C.V.: Liquid phase adsorption of crystal violet onto activated carbons derived from male flowers of coconut tree. J. Hazard. Mater. **136**, 800–808 (2006)

Tsang, D.C.W., Hu, J., Liu, M.Y., Zhang, W., Lai, K.C.K., Lo, I.M.C.: Activated carbon produced from waste wood pallets: adsorption of three classes of dyes. Water Air Soil Pollut. **184**, 141–155 (2007)

Vasanth Kumar, K.: Optimum sorption isotherm by linear and nonlinear methods for malachite green onto lemon peel. Dyes Pigments **74**, 595–597 (2006)

Wang, S., Li, H.: Structure directed reversible adsorption of organic dye on mesoporous silica in aqueous solution. Microporous Mesoporous Mater. **97**, 21–26 (2006)

Wang, S., Li, H., Xu, L.: Application of zeolite MCM-22 for basic dye removal from wastewater. J. Colloid Interface Sci. **295**, 71–78 (2006)

Weber, W.J., Morris, J.C.: Kinetics of adsorption on carbon solution. J. Sanit. Eng. Div. Am. Soc. Civ. Eng. **89**, 31–59 (1963)

Zhao, X.S., Lu, G.Q., Millar, G.J.: Advances in mesoporous molecular sieve MCM-41. Ind. Eng. Chem. Res. **35**, 2075–2090 (1996)